Available online at www.sciencedirect.com
ScienceDirect
Bioorganic & Medicinal Chemistry 15 (2007) 2768–2781
Bioorganic & Medicinal Chemistry

Second generation of 5-ethenylbenzofuroxan derivatives as inhibitors of *Trypanosoma cruzi* growth: Synthesis, biological evaluation, and structure–activity relationships☆

Williams Porcal,[a] Paola Hernández,[a] Gabriela Aguirre,[a] Lucía Boiani,[a] Mariana Boiani,[a] Alicia Merlino,[a] Ana Ferreira,[b] Rossanna Di Maio,[a] Ana Castro,[c,†] Mercedes González[a,*] and Hugo Cerecetto[a,*]

[a]*Departamento de Química Orgánica, Facultad de Química-Facultad de Ciencias, Universidad de la República, 11400 Montevideo, Uruguay*
[b]*Cátedra de Inmunología, Facultad de Química-Facultad de Ciencias, Universidad de la República, 11400 Montevideo, Uruguay*
[c]*Instituto de Química Médica (CSIC), Juan de la Cierva 3, 28006 Madrid, Spain*

Received 1 August 2006; revised 6 December 2006; accepted 1 January 2007
Available online 12 January 2007

Abstract—In vitro growth inhibitory activity of 21 new 5-ethenylbenzofuroxan derivatives against the protozoan parasite *Trypanosoma cruzi*, the causative agent of American trypanosomiasis, was studied. The designed compounds possess the previously described exigencies for optimal anti-parasite activity, the 5-ethenylbenzofuroxanyl moiety with different substituents. The synthetic key for preparing the derivatives was the Wittig procedure, that when 5-formylbenzofuroxan was used as the electrophile the corresponding deoxygenated products were marginally generated. Four of the new derivatives displayed remarkable in vitro activities against the epimastigote form of three strains of *T. cruzi*, Tulahuen 2, CL Brener, and Y. While the three deoxygenated analogues biologically assayed resulted inactives. Unspecific cytotoxicity was evaluated using human macrophages and active derivatives were not toxic at a concentration at least 13 times that of its IC_{50} against *T. cruzi* (CL Brener strain). From the preliminary structure–activity relationship studies lipophilicity and electronic requirements were found relevant to anti-*T. cruzi* activity. Active compounds are more lipophilic than inactive ones and it was also identified that an optimum value of *R* Swain-Lupton's descriptor is required for optimal activity.
© 2007 Elsevier Ltd. All rights reserved.

1. Introduction

Chagas' disease or American trypanosomiasis is an important health problem that affects around 20 million people in Central and South America. Around 2–3 million individuals develop the typical symptoms of this disease that results in 50,000 yearly deaths.[1,2] The causative agent of this disease is the hemoflagellate protozoan *Trypanosoma cruzi* (*T. cruzi*).

Trypanosoma cruzi is transmitted in rural areas to humans and other mammals by reduviid bugs such as *Rhodnius prolixus* and *Triatoma infestans*.[3] The main route of transmission is the result of blood-sucking activity of Chagas' disease vectors on mammals when feeding in a cyclic process. The parasite presents different morphological forms in a complex life cycle: amastigote, the mammalian multiplicative intra-cellular form; trypomastigote, the non-dividing bloodstream form that invades tissues; metacyclic trypomastigotes, the non-dividing highly infective form that invades mammalian tissues via wounds provoked by vector blood sucking action; epimastigotes, the replicative form that exists in the Chagas' disease vector. Recently, the existence of the epimastigote form as an obligate mammalian intra-cellular stage has been revisited[4,5] and confirmed.[6] Despite the progress achieved in the study of *T. cruzi* biochemistry and physiology, in which several crucial enzymes for parasite survival, absent in the host, have

Keywords: Ethenylbenzofuroxans; Wittig reaction; *T. cruzi*.
☆ Part of this research is presented in the Uruguayan patent of invention: Cerecetto, H.; Di Maio, R.; González, M.; Porcal, W.; Denicola, A. UR Patent No 28.019, 2003: Derivados de 5-etenilbenzofuroxano, procedimiento de preparación y utilización.
* Corresponding authors. Tel.: +598 2 5258618x216; fax: +598 2 525 07 49 (H.C.); e-mail: hcerecet@fq.edu.uy
† Present address: Neuropharma S.A. Avda. de la Industria, 52. Parque Tecnológico de Madrid, Tres Cantos, 28760 Madrid, Spain.

0968-0896/$ - see front matter © 2007 Elsevier Ltd. All rights reserved.
doi:10.1016/j.bmc.2007.01.009

been identified as potential targets for the design of new drugs,[7,8] the chemotherapy to control this parasitic infection remains undeveloped. The pharmacology is based on old and quite unspecific drugs associated with long-term treatments that give rise to severe side effects. In fact, although Nifurtimox (4-([5-nitrofurfurylidene]-amino)-3-methylthio morpholine-1,1-dioxide, Nfx, Fig. 1) and Benznidazole (*N*-benzyl-2-nitro-1-imidazoleacetamide, Bnz, Fig. 1), the only two drugs currently in use for clinical treatment of this disease, are able to wipe out parasitemia and to reduce serological titers, they are not specific enough to all *T. cruzi* strains and they do not guarantee complete cure. Both drugs act via the reduction of the nitro group. In the case of Nfx, reduction generates an unstable nitro anion radical which produces highly toxic reduced oxygen species. Whereas, Bnz involves covalent modification of macromolecules by nitro reduction intermediates.[9] The side effects of these drugs result from the oxidative or reductive damage in the host's tissues and are thus inextricably linked to its anti-parasitic activity. Despite these limitations, some studies involving nitroimidazole derivatives have been recently described.[10,11] Other drugs have been evaluated as anti-*T. cruzi* agents in the last years, among them the antifungals Ketoconazole (Ktz, Fig. 1) and Terbinafine (Tbf, Fig. 1) have demonstrated to act as *T. cruzi* membrane sterol inhibitors.[7]

We have shown that benzofuroxan derivatives (Fig. 2) possess high in vitro anti-*T. cruzi* activity against Tulahuen 2 strain[12–15] and we have demonstrated that this family of compounds produce free radicals intra-parasitically.[16] Electronic properties of the compounds play an important role on their effectiveness as anti-*T. cruzi* agents.[15,17,18] Compounds **1**–**5** are good examples of the previously reported 3-D QSAR models using in vitro anti-*T. cruzi* activities.[15] From these previous biological results new lead compounds were identified. 5-Ethenyl derivatives of benzofuroxan were more active than the other benzofuroxans studied, thus we decided to prepare new derivatives containing the ethenyl moiety on the heterocyclic system (Fig. 2).

In the present work, the development of new 5-ethenylbenzofuroxanyl derivatives (**6**–**22**, Figs. 4–8) and some deoxygenated analogues and their anti-*T. cruzi* activities are described. Unspecific mammal cytotoxicity of some selected derivatives, and the parent compounds **1** and **2**, was evaluated in vitro against human macrophages THP-1. Theoretical studies were developed in order to obtain insight into the structural requirements for optimum activity.

2. Methods and results

2.1. Synthesis

Two different general Wittig procedures were employed to prepare the 5-ethenyl derivatives (Fig. 3). In the first case (Fig. 3a), the Wittig reactions were performed using 5-formylbenzofuroxan as electrophile and the

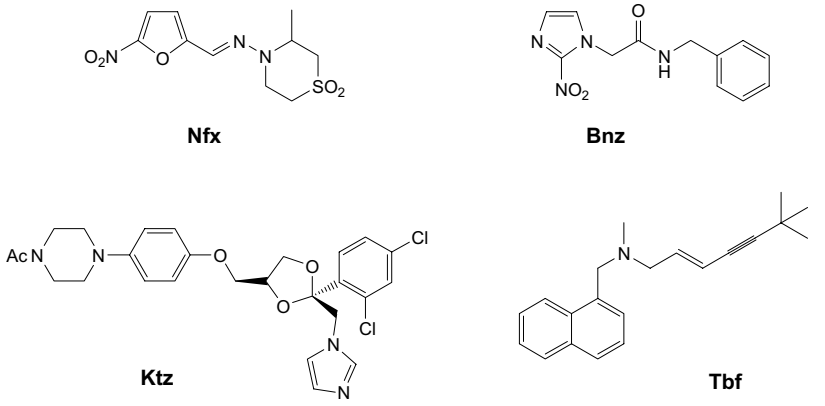

Figure 1. Drugs used clinically and experimentally as anti-*T. cruzi* agents.

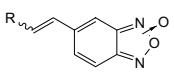

Ref.	-R	Isomeric geometry	IC_{50}[a] (μM)
1	-Ph	*E*	10.8
		Z	7.0
2	-*p*-Cl-Ph	*E*:*Z* (1:1)	4.3
3	-*p*-CF_3-Ph	*E*:*Z* (1:1)	9.8
4	-*p*-NO_2-Ph	*Z*	7.2
5	-H	-	> 25.0

[a] In vitro activity on *T. cruzi* (Tulahuen 2 strain).

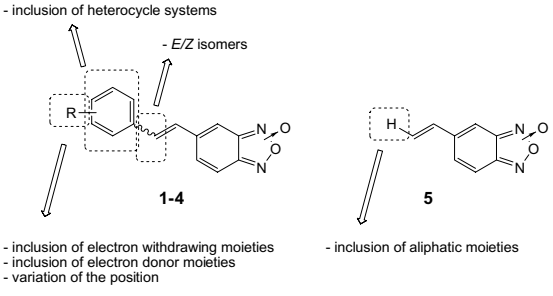

Figure 2. Parent benzofuroxan, anti-*T. cruzi* activity[14,15] and designed structural modifications.

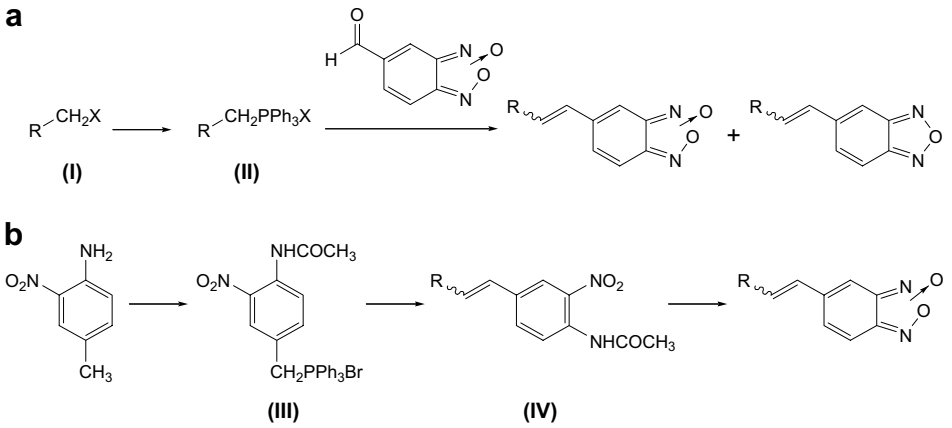

Figure 3. General procedures used to prepare desired derivatives.

corresponding phosphonium salts, **II**, prepared from the halide **I**. Deoxygenated analogues were marginally generated in these olefination reactions eventhough Boden's mild conditions were used.[19] The second approach (Fig. 3b), designed to avoid the *N*-oxide reduction in the olefination conditions, involved the use of the phosphonium salt **III** that was reacted with the corresponding aldehydes. Further, hydrolysis and oxidation in one-pot[20] produced the desired products in good yield.

Derivatives of the series of 5-(phenylethenyl) benzofuroxan with mesomeric electron donor moieties in the phenyl substituent were prepared using the procedures shown in Figure 4. Derivatives **6** and **7** were prepared following the general procedure shown in Figure 3a. For derivative **6** it was possible to isolate geometric isomers, namely **6*E*** and **6*Z***, and the corresponding deoxygenated analogues, **6*E*d** and **6*Z*d**. For derivative **7** only the *E* isomer was obtained although the deoxygenated derivative was chromatographically observed as a fluorescent spot. But it was not isolated in the chromatographic purification process from the reaction mixture.

In order to avoid the formation of secondary products, the methodology depicted in Figure 3b was assayed in the derivative **8**'s preparation. The reaction between the phosphonium salt **III** and the poor electrophile *p*-dimethylaminobenzaldehyde, in the typical Boden's conditions, yielded the phosphonium salt's hydrolysis product (Fig. 4b).[21,22] In order to diminish this undesirable reaction, strong base, *t*-BuOK, and higher temperature, boiling toluene, were employed yielding the desired alkene **IVa** as a mixture of geometric isomers. Attempts to transform **IVa** into **8** using one-pot hydrolysis/oxidation procedure were unsuccessful. Finally, derivative **8** was obtained as *E* isomer (Fig. 4b) from the phosphonium salt **IIc** and 5-formylbenzofuroxan.[23] Marginally deoxygenated derivative, **8*E*d**, was generated and it was isolated and spectroscopically characterized.

In the synthesis of *p*-hydroxy derivative **9** (Fig. 4c) was employed the phosphonium salt **IId**[23] reacting with 4-chloro-3-nitrobenzaldehyde. Then the *E*-alkene **V** was converted into **9*E*** by reaction with sodium azide in one-pot S_NAr/cyclization procedure.

Derivatives of the series of 5-(phenylethenyl) benzofuroxan with mesomeric electron withdrawing moieties in the phenyl substituent were prepared as depicted in Figure 5. Derivatives **10** and **11** were prepared from the corresponding phosphonium salt (**IIe** and **IIf**) and 5-formylbenzofuroxan, both derivatives were obtained as chromatographically separable *E* and *Z* isomers. In both cases the reduced derivatives were observed but they were not isolated. The preparation of the *o*-nitro derivative **12** was done following the general procedure shown in Figure 3b. The alkenes (**IVb*E*** and **IVb*Z***) were submitted, independently, to hydrolysis/oxidation process to yield both geometric isomers, namely **12*E*** and **12*Z***.

The two new halo derivatives developed, **13** and **14**, are shown in Figure 6. The *m*-fluoro derivative **13** was prepared using the Wittig–Boden process with 5-formylbenzofuroxan as electrophile, observing the formation of the deoxygenated analogues which were not isolated. The desired product was obtained as the chromatographically inseparable mixture of geometric isomers, namely **13*E*/*Z***, in a proportion *E*:*Z* = 1:1. For the *p*-bromo derivative **14** was successfully assayed the general methodology shown in Figure 3b. As in the preparation of derivative **8** (Fig. 4b), the reaction between the phosphonium salt **III** and *p*-bromobenzaldehyde in Boden's conditions yielded the phosphonium salt's hydrolysis product (Fig. 6b). So, stronger conditions were employed generating the inseparable mixture of *E* and *Z* isomer alkenes, **IVc**, that were submitted to the hydrolysis/oxidation process to yield the desired product as the *E* isomer.

Three different derivatives of parent compound **5** (Fig. 2), where non-aromatic substituents were included in the ethenyl moiety, were developed as shown in Figure 7. While derivative **15** was isolated as the geometric isomeric mixture, **15*E*/*Z***, the stabilized phosphonium salt methyloxycarbonyl methyl triphenyl phosphonium bromide **IIi** generated exclusively the *E* isomer, namely

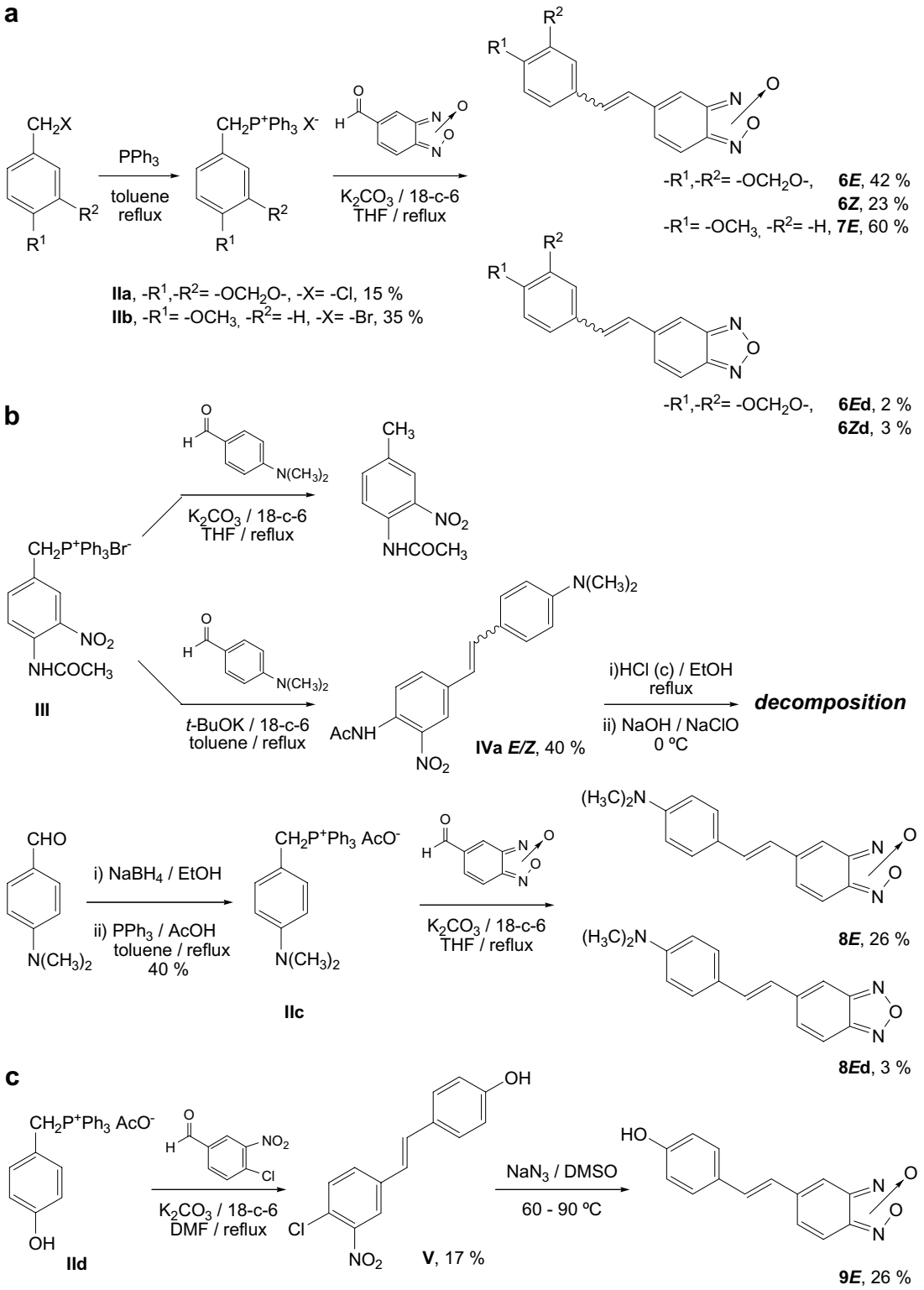

Figure 4. Series of 5-(phenylethenyl)benzofuroxan with mesomeric electron donor moieties in the phenyl substituent.

16*E*. Derivative **17** was obtained following the other methodology where the phosphonium salt **III** was reacted with *n*-pentanal yielding the chromatographically inseparable mixture of alkenes **IVd** that after hydrolysis/oxidation generated the desired product as the isomeric mixture **17*E*/*Z*** in a proportion *E*:*Z* = 1:1.

Furthermore, heterocyclic analogues of parent compounds **1** and **4** (Fig. 2) were prepared as shown in Figure 8. Derivatives **18**–**21** were prepared from the phosphonium salt **III** (Fig. 3a and b), yielding the alkenes with different isomeric distribution. In the case of the thienyl derivative, intermediate **IVe *E*** was generated maintaining this

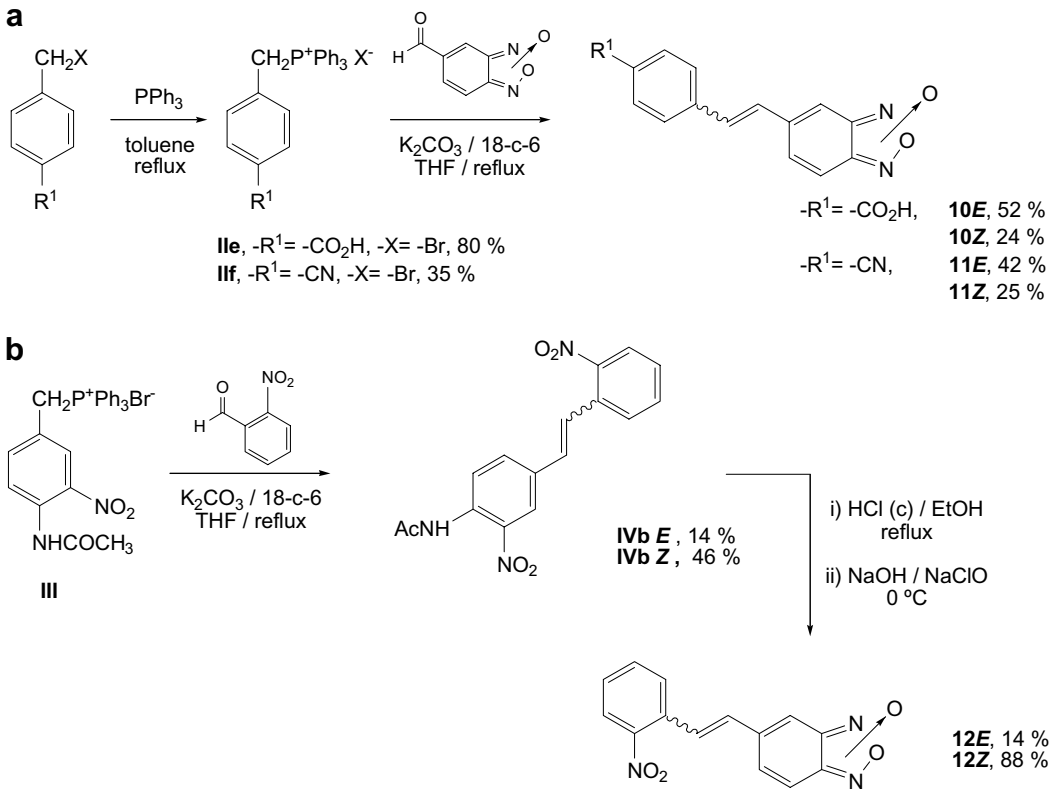

Figure 5. Series of 5-(phenylethenyl)benzofuroxan with mesomeric electron withdrawing moieties in the phenyl substituent.

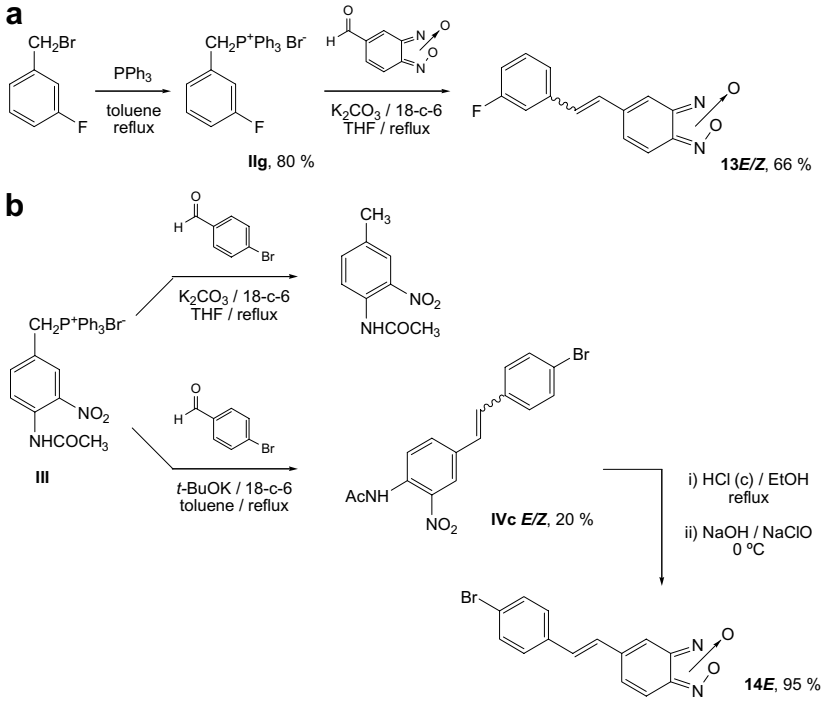

Figure 6. Series of 5-(phenylethenyl)benzofuroxan with halogen in the phenyl substituent.

isomeric distribution after the hydrolysis/oxidation reaction. However, for the 5-nitrothienyl analogue the intermediate was produced as the *Z* isomer (**IVf *Z***) that after the hydrolysis/oxidation reaction changed the geometric distribution to the most stable isomer, product **19*E***. In the reaction between 5-formylbenzofuroxan and phosphonium salt **III** the *Z* isomer was generated, namely **20*Z***, and after the one-pot process the geometric

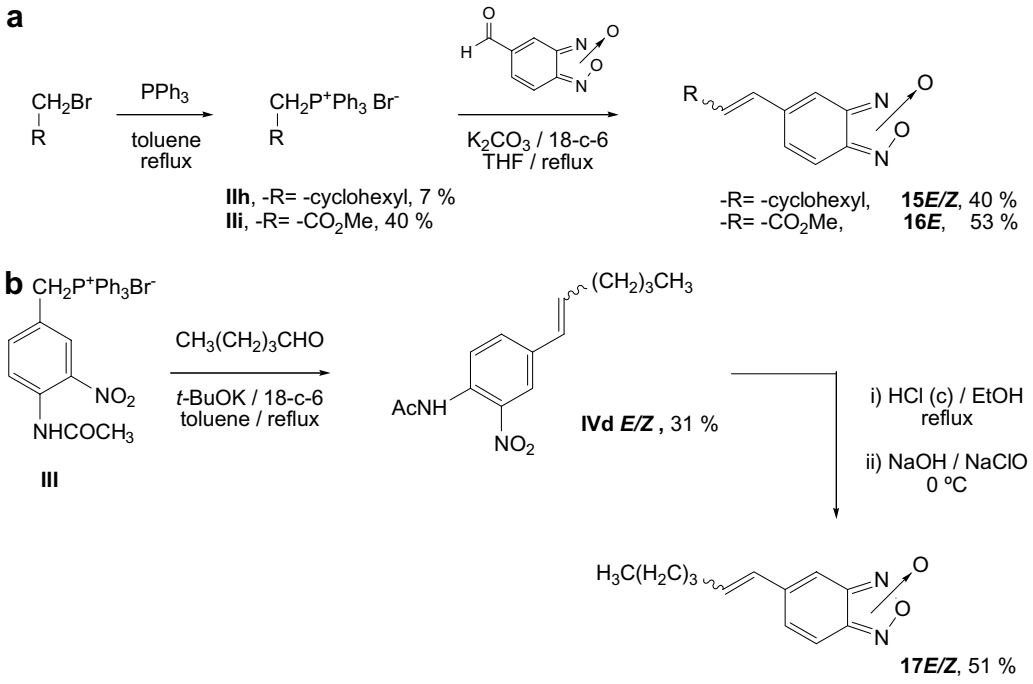

Figure 7. Series of 5-ethenylbenzofuroxan with non-aromatic substituent in the ethenyl moiety.

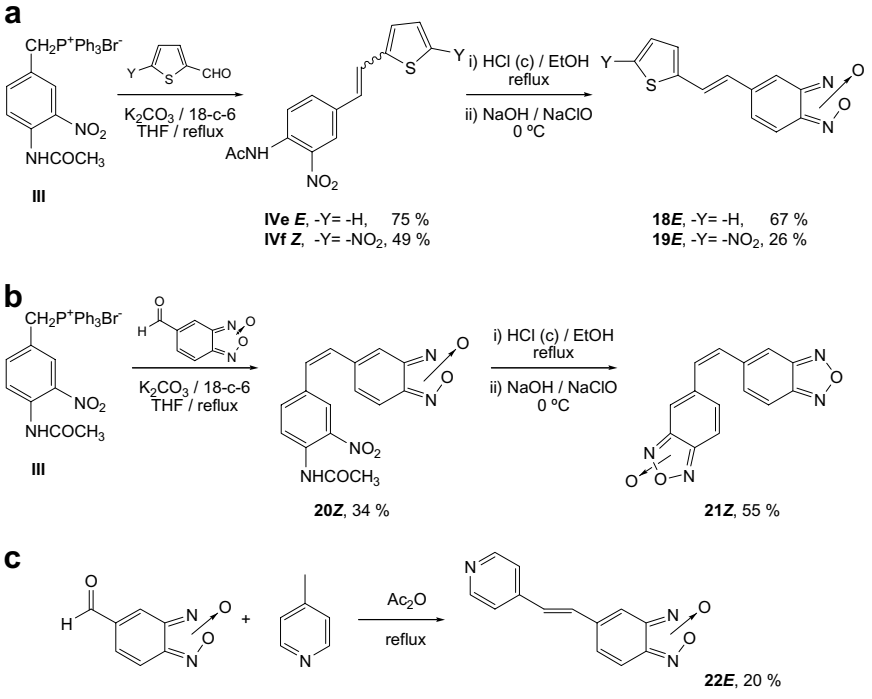

Figure 8. Series of 5-ethenylbenzofuroxan with heterocyclic substituent in the ethenyl moiety.

distribution was conserved however the *N*-oxide reduction was observed. A detailed study showed that the *N*-oxide moiety was lost after hydrolysis conditions (HCl (concd)/EtOH/reflux). For the preparation of the 4-pyridinyl derivative, the acidity of methyl protons of 4-picoline was used. In the conditions depicted in Figure 8c, the *E* isomer of derivative **22** was generated with a low proportion of the deoxygenated analogue.

All new compounds were characterized by NMR (^{1}H, ^{13}C, COSY, and HETCOR experiments), IR, and MS. The purity was established by TLC and microanalysis. The stereochemistry around olefinic carbon–carbon bond was established using the corresponding ^{1}H NMR coupling constant. It is well established that benzofuroxan derivatives exist at room temperature as a mixture of tautomers (i.e., Fig. 9a). The benzo

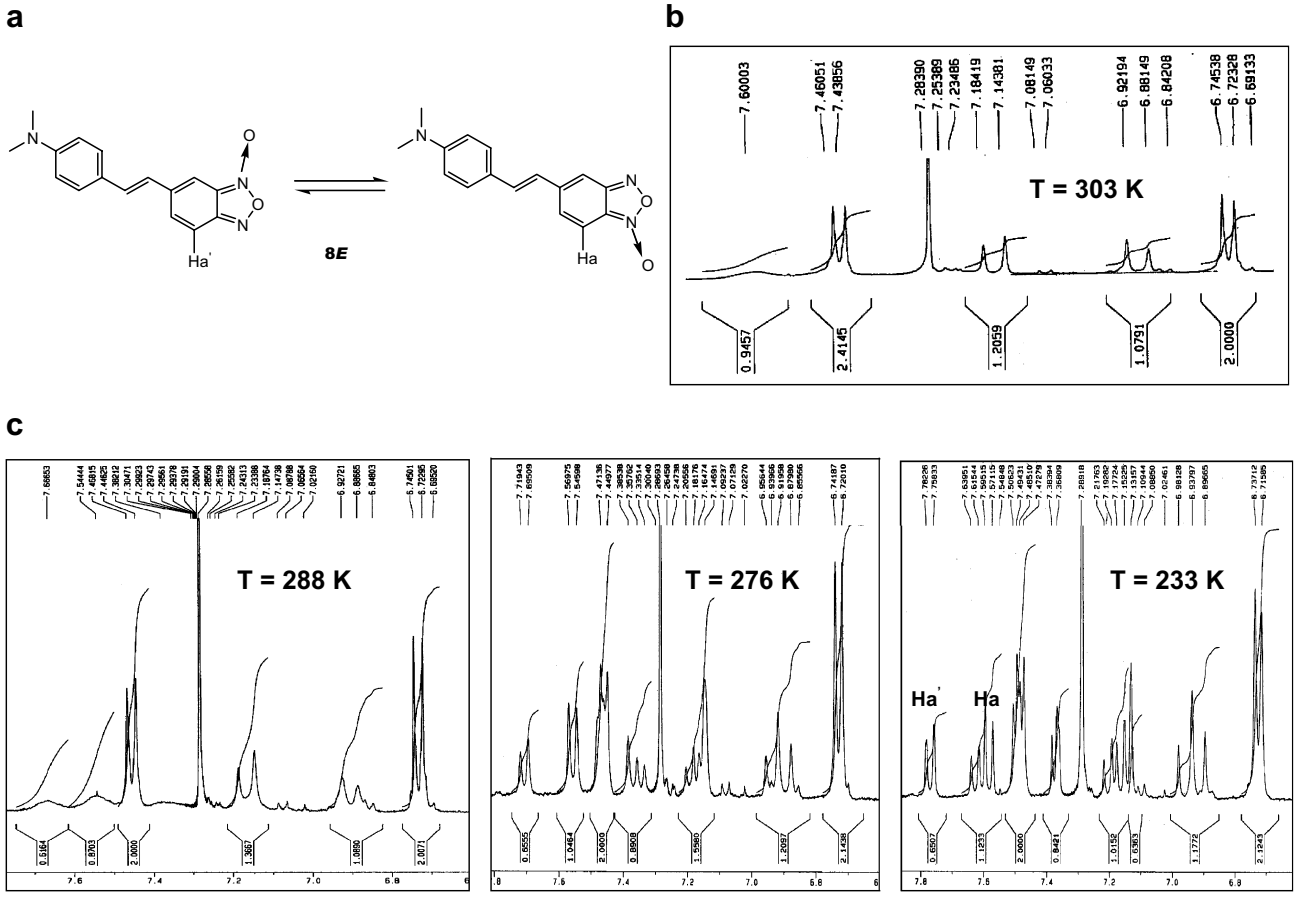

Figure 9. (a) Tautomeric equilibrium of derivative **8*E***. (b) ^{1}H NMR spectra of **8*E*** in $CDCl_3$ at 303 K. (c) Series of ^{1}H NMR spectra of **8*E*** in $CDCl_3$ at different temperatures.

substituent could occupy the 5- or 6-position and the proportion of both tautomers in the equilibrium depends on the electronic characteristic of the substituent.[24] At room temperature (303 K) ^{1}H and ^{13}C NMR spectra of the benzofuroxans showed broad signals due to the rapid tautomeric equilibrium (i.e., Fig. 9b). When NMR experiments were carried out at low temperature (e.g., 233 K), the aromatic region showed narrow peaks corresponding to both tautomers (Fig. 9c).[15,18,25,26] In chloroform solution, (approximately 10% w/v) at 303 K, compound **8*E*** shows broad resonance signals due to incomplete coalescence (Fig. 9b). While, on cooling, the broad signals were resolved below 270 K and at 233 K it was possible to record the complete series of spectra (^{1}H, ^{13}C NMR, and HMQC, HMBC, and COSY experiments). The ratio of 5- and 6-tautomer could be determined at low temperature using specific chemical shifts. For example at 233 K, in $CDCl_3$, the chemical shifts of protons Ha and Ha′ (see Fig. 9a and c) allow us to determine the tautomeric proportion that resulted 5-tautomer:6-tautomer = 42:58.

2.2. Biological characterization

2.2.1. In vitro anti-trypanosomatid activity. The new benzofuroxan derivatives were tested in vitro against three different strains of *T. cruzi*, Tulahuen 2, CL Brener, and the Nfx and Bnz partially resistant strain, Y strain.[27,28] The in vitro studies were completed for the parent compounds **1**–**4**[14,15] testing them against Brener and Y strains. As a first screening the compounds were incorporated into the media at 25 μM and their ability to inhibit the growth of the epimastigote form of the parasite, percentage of growth inhibition, was evaluated in comparison to the control (no compound added to the media) at day 5. Nfx, Bnz, Ktz, and Tbf were used as the reference trypanocidal drugs. In order to confirm the relevance of the *N*-oxide moiety in the activity, deoxygenated analogues were included in the biological studies. The IC_{50} concentration (which causes a 50% reduction in parasite growth) was assessed for the most active derivatives (Table 1).

2.2.2. In vitro mammal cytotoxicity. Unspecific mammal cytotoxicity of some selected benzofuroxans was evaluated in vitro at 25–400 μM, using THP-1 human macrophages as the cellular model (Table 2).[29] In the study, parent compounds **1** and **2**, as pure isomers and as geometric isomeric mixtures, and trypanocidal agents Ktz and Tbf were included.

2.3. Structure–activity relationships

First, 12 substituted-phenylethenyl benzofuroxans were used in the structure–activity relationship studies, the parent compounds **1**–**4** and the new derivatives **6**–**11**,

Table 1. In vitro biological activity of parent compounds, new benzofuroxan derivatives, Nfx, Bnz, Ktz, and Tbf

Compound	Ref.	Nfx	Bnz	Ktz	Tbf	1		2	3	4	5	6		6d		7	8	8d
	Isomer					*E*	*Z*	*E*:*Z*	*E*:*Z*	*Z*	—	*E*	*Z*	*E*	*Z*	*E*	*E*	*E*
IC_{50} (μM)[a,b]	T2[c]	7.7	7.4	10.0	17.1	10.8	7.0	4.3	9.5	7.0	>25.0	5.3	2.9	>25.0	>25.0	8.0	15.7	>25.0
	CLB[d]	8.5	4.5	5.0	42.0	7.5	15.7	7.5	4.5	10.5	—[e]	9.0	9.0	>25.0	>25.0	5.0	4.4	>25.0
	Y[f]	6.5	3.8	9.8	44.7	6.2	9.0	9.0	10.0	13.5	—	7.3	8.5	>25.0	>25.0	8.5	22.0	—

Compound	Ref.	9	10		11		12		13	14	15	16	17	18	19	20	21	22
	Isomer	*E*	*E*	*Z*	*E*	*Z*	*E*	*Z*	*E*:*Z*	*E*	*E*:*Z*	*E*	*E*:*Z*	*E*	*E*	*Z*	*Z*	*E*
IC_{50} (μM)[a,b]	T2	10.2	>25.0	>25.0	>25.0	>25.0	26.4	24.4	2.5	8.7	13.6	>25.0	19.7	0.6	6.0	24.0	>25.0	15.0
	CLB	22.5	—	—	—	—	11.1	13.7	10.0	2.5	—	—	12.8	15.0	3.5	—	—	—
	Y	25.0	—	—	—	—	—	—	7.5	5.5	—	—	—	12.2	4.5	—	—	24.0

[a] IC_{50}, concentration that causes a 50% reduction in parasite growth.
[b] The results are means of three different experiments with a SD less than 10% in all cases.
[c] T2, Tulahuen 2 strain.
[d] CLB, CL Brener strain.
[e] Not determined.
[f] Y, Y strain.

Table 2. Cytotoxicity of benzofuroxan derivatives, reduced analogues, and reference compounds to THP-1 human macrophages

Compound	THP-1 IC_{50} (μM)[a,b]	$IC_{50,macrophage}$/$IC_{50,epimastigote}$		
		T2[c]	CLB[d]	Y[e]
1*E*	109.9	10.2	14.7	17.7
1*Z*	62.6	8.9	4.0	7.0
1*E*:*Z*(1:1)	149.0	—[f]	—	—
2*E*	>200.0[g]	—	—	—
2*Z*	97.0	—	—	—
2*E*:*Z*(1:1)	66.7	15.5	8.9	7.4
6*E*	220.0	41.5	24.4	30.1
6*Z*	120.0	41.4	13.3	14.1
6*E*:*Z*(1:1)	81.0	—	—	—
6*Z*d	>400.0	<40	<40	<40
8*E*	>400.0	>25	>90	>18
Ktz	44.0	4.4	8.8	4.5
Tbf	329.3	19.3	7.8	7.4

[a] IC_{50}, concentration that produces a 50% reduction in cell viability.
[b] The results are means of two different experiments with a SD less than 10% in all cases.
[c] T2, Tulahuen 2 strain.
[d] CLB, CL Brener strain.
[e] Y, Y strain.
[f] Not determined.
[g] Solubility problems.

13, and **14**. For derivatives **1**, **6**, **10**, and **11** the biological activities of the *E* isomeric forms were considered. The IC_{50} in Tulahuen 2 strain was used as the biological activity. $\log_{10}$ (IC_{50}) was used as the dependent variable in the linearization procedure. In the equations *n* represents the number of data points, r^2 is the correlation coefficient, *s* is the standard deviation of the regression equation, and *F* value is related to the *F*-statistical analysis (Fischer test). As the independent variables were employed the previously tabulated substituent constants related to the electronic, the lipophilic, and the steric properties (Hammett constants σ_m, σ_p, Swain-Lupton's constants *F* and *R*, lipophilic constant π, and molar refractivity MR).[30,31] One-variable and multivariable regressions between the activity and the physicochemical descriptors were studied. Eq. 1 shows the best one-variable relationship obtained where activity is correlated, in a quadratic manner, with the Swain-Lupton's constant *R* (Fig. 10).

$$\log_{10}(IC_{50}) = 0.95(\pm 0.09) + 1.34(\pm 0.49)R + 1.71(\pm 0.63)R^2$$
$$n = 12, r = 0.680, s = 0.256, F = 3.88, p = 0.061. \quad (1)$$

This discrete result could be modestly improved, in the r^2 correlation coefficient, including lipophilic descriptor in the analysis ($r = 0.700$, $s = 0.298$, $F = 2.58$, $p = 0.128$). Although the other statistical parameters (*s*, *F*, and *p*) diminished their quality in this correlation, it shows the relevance of lipophilicity in the biological activity. Similarly, molar refractivity (MR) could be studied together with *R* and R^2 however the quality of the statistical correlation resulted worse than the statistical parameters obtained in Eq. 1 ($r = 0.681$, $s = 0.272$, $F = 2.30$, $p = 0.154$). Again, the participation of this descriptor showed the relevance of substituent volume in the bio-response. Besides, the correlation matrix for the used physicochemical descriptors was performed and cross-correlations between the descriptors were not obtained. Thus, these parameters are orthogonal, allowing its safe use in the multilinear regression relationship.[32,33]

In order to include in the SAR study all the developed benzofuroxan derivatives, molecular modeling studies were performed by calculating their stereoelectronic properties. These properties were determined using DFT calculations.[34,35] A detailed conformational search for each of the molecules was performed, using MM methods, to find the minimum energy and highest abundance conformer. The geometry of this conformer was fully optimized by applying B3LYP/6-31G*//AM1 in the gas phase that allows us to obtain acute results with low time of computational calculi. Then, single point B3LYP/6-31G* calculation was performed.[36–38] The

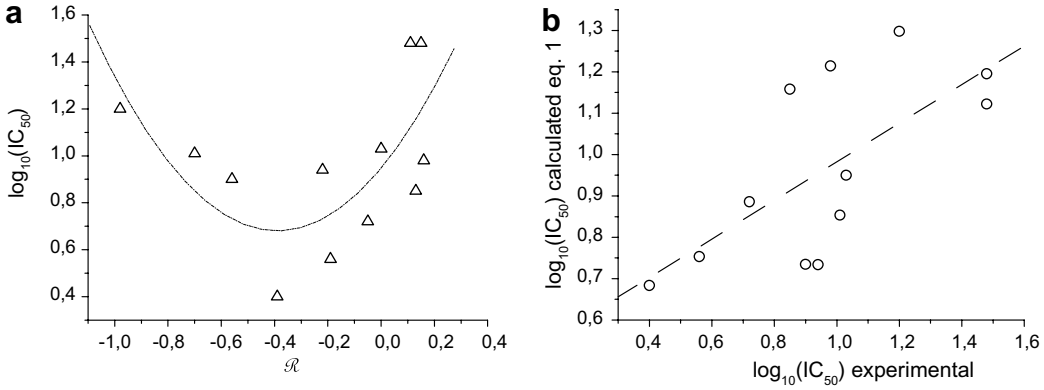

Figure 10. (a) R versus $\log_{10}(IC_{50})$. (b) Plot of $\log_{10}(IC_{50})$ experimental versus calculated values from Eq. 1. IC_{50} refers to results on Tulahuen 2 strain.

Table 3. Results of the t-test analysis performed on the two benzofuroxan populations, actives and inactives, and on the corresponding two populations of studied theoretical descriptors (clog$P$ and gap)

Compound	IC_{50}[a]		clog P		Gap	
Most actives	Mean = 6.2	$t = 6.56$, $p = 2.2 \times 10^{-6}$	Mean = 4.49	$t = 2.08$, $p = 0.05$	Mean = 2.97	$t = 2.06$, $p = 0.05$
Less actives	Mean = 22.9		Mean = 3.82		Mean = 3.10	

[a] For compounds with $IC_{50} > 25.0$ μM it was used $IC_{50} = 30.0$ μM in this study.

properties determined and examined in this study were total energy, magnitude of dipolar moment, HOMO's and LUMO's energies, gap (E_LUMO–E_HOMO), volume, and the logarithm of the partition coefficient of the non-ionized molecules (log P). Theoretical log P (clog P) was calculated using the Villar method, implemented in PC SPARTAN 04 package[39] at the AM1 semiempirical level. Non-statistical significant correlations were obtained when the different theoretical descriptors were studied as independent variable, but a clear tendency was observed between activities and clog P, the most active compounds possess the highest clog P, or activities and gap, the most active compounds possess in general the lowest gap. These facts were studied dividing the benzofuroxans into two groups of compounds, the most actives against Tulahuen 2 strain ($IC_{50} < 11$ μM) and the less actives against the parasite ($IC_{50} \geqslant 11$ μM). These two groups of activities resulted significantly different at 2.2×10^{-6} level (Table 3). Then, the corresponding two groups of clog P or gap, for the most and less active derivatives, were submitted to a t-test analysis. The clog P values, for both pre-defined populations of compounds, resulted significantly different at a 0.05 level and the gap values at a level lower than 0.05. Figure 11 shows, graphically, the distribution of the HOMO and the LUMO maps in some relevant benzofuroxans. In these graphics it is possible to observe the differences in the LUMO distributions between active and inactive derivatives against Tulahuen 2 strain (Fig. 11a). The LUMO is located at the heterocyclic carbons for the active derivatives (see arrows in Fig. 11a) and at the olefinic carbons for the inactive ones. While the HOMO distributions show less differences between active and inactive derivatives (Fig. 11b).

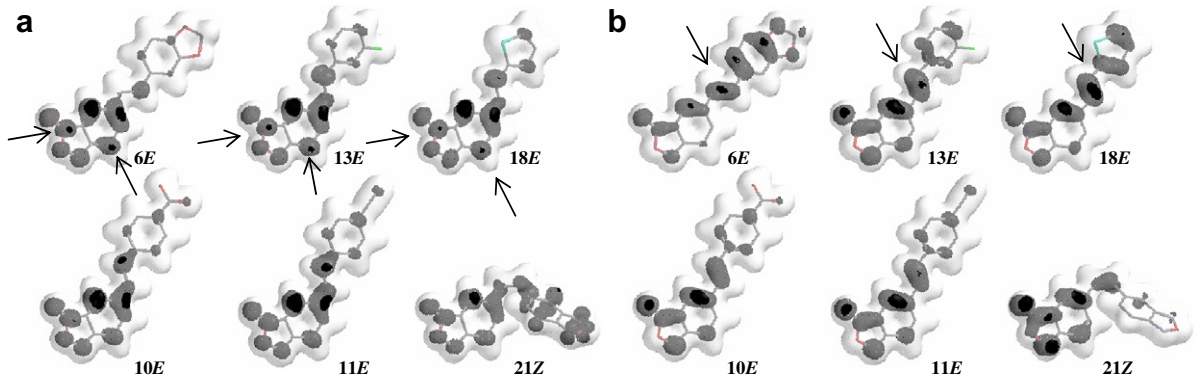

Figure 11. (a) Electron density (transparent gray, isovalue 0.02) and LUMO (solid black, isovalue 0.039) isosurfaces for active (up) and inactive derivatives (down), against Tulahuen 2 strain. (b) Electron density (transparent gray, isovalue 0.02) and HOMO (solid black, isovalue 0.039) isosurfaces for active (up) and inactive derivatives (down), against Tulahuen 2 strain.

3. Discussion

In this second generation of 5-ethenylbenzofuroxan derivatives were found excellent anti-*T. cruzi* agents. It was not possible to observe different susceptibilities of the benzofuroxans against the three studied strains resulting, in general, equally active in the three strains. On the other hand, clear differences were not observed in the activities between the different isomeric forms of the alkenes. The most active derivatives, **6**, **13**, **14**, and **19**, displayed good to excellent IC_{50} against the three strains and in the same order as the IC_{50} of clinical drugs Nfx and Bnz. The halo derivatives **13** and **14** possess better activities than the parent compound, the chloro-derivative **2**, being the fluoro-analogue **13** one of the most active developed benzofuroxans against Tulahuen 2 strain and the bromo-analogue **14** the most active against CL Brener strain. The derivative **6** with an electron-donor substituent, in both isomeric forms, possesses good capacity to inhibit the three studied strains. The 5-nitrothienyl derivative **19** shows excellent activity against CL Brener and Y, and good activity against Tulahuen 2 strain. The thienyl derivative, **18**, is the best compound against Tulahuen 2 strain, with acceptable IC_{50} against the two other evaluated strains. As previously, it was evidenced[12–15,40,41] that the deoxygenated analogues result inactives showing the relevance of the *N*-oxide moiety in the anti-*T. cruzi* activity. In general, the electron-withdrawing substituted derivatives result inactives against the epimastigote form of the parasite. The derivatives substituted in the ethenyl moiety by a non-aromatic group, like **15** and **17**, possess medium activity showing that aromatic moieties are not fundamental for adequate anti-parasite activity. According to the mammal cytotoxicity studies, the benzofuroxan parents and new derivatives result selective against the parasite. *Z* stereoisomers were more toxic than the *E* analogues, maybe as a consequence of their best solubilities in the biological medium. The new derivatives were less toxic than the parent compounds. Remarkably, the electron-donor derivatives, compounds **6**, in both stereoisomeric forms, and **8*E*** showed low mammal cytotoxicity at a concentration that was at least 25 times that of its IC_{50} against *T. cruzi* epimastigotes (Tulahuen 2 strain). The corresponding deoxygenated derivative, **6*Z*d**, resulted non-toxic in the assayed conditions ($IC_{50,macrophage} > 400.0$ μM) however its *T. cruzi* activity is very low.

The performed SAR studies showed that in the series of substituted-phenylethenyl derivatives some electronic requirements are needed for a good activity. According to Eq. 1 optimum value of *R* Swain-Lupton's descriptor is required for optimal activity. Substituent volume and lipophilic characteristics of phenyl's substituents could play some role in the activity but not good statistical results were obtained between these descriptors and bio-response. The study of all the population, using molecular modeling, enables to identify some tendency between the theoretically studied properties and bio-activity. In one hand, more lipophilic compounds result more active than less lipophilic benzofuroxans. On the other hand, some electronic requirement was evidenced in terms of gap (E_LUMO–E_HOMO) the most active derivatives possessing the lowest gap. Further, the most reactive derivatives with lowest gaps are the most active against *T. cruzi*. Analyzing the gap's effect in the activity we studied the localization of frontier molecular orbitals, HOMO and LUMO, in some selected derivatives. It is possible to observe that nitrogen 1 and carbon 4 of the benzofuroxanyl system contribute to the LUMO of active derivatives (arrows in Fig. 11a). This fact could be involved in some differential nucleophilic or electronation processes. In reference to the HOMO's contribution, the clearest difference is related to the contribution of the olefinic carbons in the active benzofuroxans (arrows in Fig. 11b). Maybe, this region interacts with a specific counterpart in a biological receptor.

4. Conclusions

The results presented above indicate that the in vitro activity of new 5-ethenylbenzofuroxanyl derivatives against *T. cruzi* epimastigotes is superior to that of the first generation members possessing lower mammalian cytotoxicity. These results provide supporting evidence for further in vivo studies of these compounds in appropriate animal models for Chagas' disease.

5. Experimental

5.1. Chemistry

All starting materials were commercially available research-grade chemicals and used without further purification. Compounds **1*E***, **1*Z***, **2*E*:*Z***, **3*E*:*Z***, **4*Z***, 5-formylbenzofuroxan, and the phosphonium salts **IIc**, **IId**, and **III** were prepared following literature procedures.[14,15,23] The purity of the intermediates **II**, **IV** and compound **V** was established by ^{1}H NMR analysis. All solvents were dried and distilled prior to use. All the reactions were carried out in a nitrogen atmosphere. The typical work-up included washing with brine and drying the organic layer with sodium sulfate before concentration in vacuo. Melting points were determined using a Leitz Microscope Heating Stage Model 350 apparatus or a Mettler FP82 + FP80 apparatus and are uncorrected. Elemental analyses were obtained from vacuum-dried samples (over phosphorus pentoxide at 3–4 mm Hg, 24 h at room temperature) and performed on a Fisons EA 1108 CHNS-O analyser. Infrared spectra were recorded on a PerkinElmer 1310 apparatus, using potassium bromide tablets; the frequencies are expressed in cm^{-1}. ^{1}H NMR spectra were recorded on a Bruker DPX-400 (at 400 MHz) instrument, with tetramethylsilane as the internal reference and in the indicated solvent; the chemical shifts are reported in ppm. *J* values are given in Hz. The ^{1}H NMR signals reported were obtained at 303 K. Mass spectra were recorded on a Shimadzu GC-MS QP 1100 EX instrument, using electronic impact at 70 eV.

5.2. General procedure for the synthesis of phosphonium salts (II)

A mixture of triphenylphosphine (1.1 equiv) and the corresponding halide (1.0 equiv) in toluene was heated at reflux for 8–12 h. Then the mixture was allowed to cool to room temperature and the white crystalline solid was collected, washed with petroleum ether and ethyl ether, and dried in vacuum.

5.3. General procedure for the synthesis of 5-ethenylbenzofuroxan derivatives 6–8, 10, 11, 13, 15, and 16

A mixture of 5-formylbenzofuroxan (1.0 equiv), the corresponding phosphonium salt **II** (1.1 equiv), K_2CO_3 (1.1 equiv), 18-crown-6 (0.01 equiv), and THF (5.0 mL/mmol) as solvent was stirred at reflux until the carbonyl compound was not present (SiO_2, petroleum ether/EtOAc (8:2)). After the work-up, the residue was purified by column chromatography (SiO_2, mixtures of petroleum ether/EtOAc).

5.3.1. 5*E*-[2-(3,4-Methylendioxyphenyl)ethenyl]benzo[1,2-*c*]1,2,5-oxadiazole N^1-oxide (6*E*). Orange-brown needles, mp 183.7–184.5 °C (from acetonitrile:water) (Found: C, 63.5; H, 3.3; N, 9.7. $C_{15}H_{10}N_2O_4$ requires C, 63.8; H, 3.6; N, 9.9); ^{1}H NMR ($CDCl_3$) δ 5.98 (s, 2H) 6.91 (d, J = 8.0, 1H), 7.16 (dd, J = 1.6, J = 7.9, 1H), 7.27 (d, J = 1.6, 1H), 7.29 (d, J = 16.3, 1H), 7.48 (d, J = 16.3, 1H), 7.50 (bs, 1H), 7.61 (bs, 1H), 7.86 (bs, 1H); MS *m*/*z* (abundance, %): 282 ($M^{+\cdot}$, 65), 266 (11), 247 (9), 222 (100), 163 (70); IR ν 1625, 1379, 1273, 1039.

5.3.2. 5*Z*-[2-(3,4-Methylendioxyphenyl)ethenyl]benzo-[1,2-*c*]1,2,5-oxadiazole N^1-oxide (6*Z*). Yellow-orange needles, mp 98.9–100.3 °C (from hexane:EtOAc) (Found: C, 63.7; H, 3.5; N, 9.7. $C_{15}H_{10}N_2O_4$ requires C, 63.8; H, 3.6; N, 9.9); ^{1}H NMR ($CDCl_3$) δ 5.98 (s, 2H), 6.50 (d, J = 12.0, 1H), 6.70 (s, 1H), 6.75 (s, 2H), 6.77 (d, J = 12.0, 1H), 7.12 (bs, 1H), 7.28 (bs, 2H); MS, *m*/*z* (abundance, %): 282 ($M^{+\cdot}$, 70), 266 (5), 247 (11), 222 (100), 163 (70); IR ν 1620, 1514, 873.

5.3.3. 5*E*-[2-(3,4-Methylendioxyphenyl)ethenyl]benzo[1,2-*c*]1,2,5-oxadiazole (6*E*d). From the chromatographic purification process of **6*E*** and **6*Z*** was also isolated the deoxygenated analogue **6*E*d**. Orange solid, mp 180.0–182.0 °C (Found: C, 67.9; H, 3.5; N, 10.1. $C_{15}H_{10}N_2O_3$ requires C, 67.7; H, 3.8; N, 10.5); ^{1}H NMR ($CDCl_3$) δ 6.03 (s, 2H), 6.87 (d, J = 8.0, 1H), 7.05 (dd,J = 1.5, J = 8.0, 1H), 7.05 (d, J = 16.0, 1H), 7.12 (d,J = 1.5 1H), 7.22 (d, J = 16.0, 1H), 7.71 (s, 1H), 7.73 (dd,J = 1.2, J = 9.5, 1H), 7.83 (d, J = 9.5, 1H); MS, *m*/*z* (abundance, %): 266 ($M^{+\cdot}$, 90), 249 (52), 236 (37), 209 (30), 177 (100); IR ν 2895, 1610, 1570, 1539, 1492, 1257, 1035, 954, 927.

5.3.4. 5*Z*-[2-(3,4-Methylendioxyphenyl)ethenyl]benzo-[1,2-*c*]1,2,5-oxadiazole (6*Z*d). From the chromatographic purification process of **6*E*** and **6*Z*** was also isolated the deoxygenated analogue **6*Z*d**. Yellow solid, mp 81.0–83.0 °C (Found: C, 67.5; H, 3.4; N, 10.3. $C_{15}H_{10}N_2O_3$ requires C, 67.7; H, 3.8; N, 10.5); ^{1}H NMR ($CDCl_3$) δ 5.97 (s, 2H), 6.59 (d, J = 12.0, 1H), 6.74 (m, 3H), 6.78 (d, J = 12.0, 1H), 7.28 (d, J = 9.7, 1H), 7.65 (d, J = 9.5, 1H), 7.69 (s, 1H); MS, *m*/*z* (abundance, %): 266 ($M^{+\cdot}$, 100), 249 (33), 236 (20), 209 (50), 177 (91); IR ν 2890, 1600, 1500, 1356, 1286, 841.

5.3.5. 5*E*-[2-(4-Methoxyphenyl)ethenyl]benzo[1,2-*c*]1,2,5-oxadiazole N^1-oxide (7*E*). Yellow solid, mp 158.0–159.0 °C (Found: C, 66.9; H, 4.3; N, 10.1. $C_{15}H_{12}N_2O_3$ requires C, 67.2; H, 4.5; N, 10.4); ^{1}H NMR ($CDCl_3$) δ 3.87 (s, 3H), 6.96 (d, J = 8.7, 2H), 6.99 (d, J = 16.0, 1H), 7.16 (d, J = 16.0, 1H), 7.51 (d, J = 8.7, 2H), 7.58 (bs, 3H); MS, *m*/*z* (abundance, %): 268 ($M^{+\cdot}$, 79), 252 (3), 208 (100), 165 (85); IR ν 1603, 1537, 960.

5.3.6. 5*E*-[2-(4-Dimethylaminophenyl)ethenyl]benzo[1,2-*c*]1,2,5-oxadiazole N^1-oxide (8*E*). Orange-brown solid, mp 150 (d) °C (Found: C, 67.9; H, 5.3; N, 14.6. $C_{16}H_{15}N_3O_2$ requires C, 68.3; H, 5.4; N, 14.9); ^{1}H NMR ($CDCl_3$) δ 3.04 (s, 6H), 6.73 (d, J = 8.8, 2H), 6.90 (d, J = 16.2, 1H), 7.16 (d, J = 16.2, 1H), 7.45 (d, J = 8.8, 2H), 7.60 (bs, 3H); MS, *m*/*z* (abundance, %): 265 ($M^{+\cdot}-16$, 6), 235 (14), 209 (2), 148 (28), 135 (57), 63 (100); IR ν 3050, 2900, 1599, 1482, 1450, 1188, 814.

5.3.7. 5*E*-[2-(4-Dimethylaminophenyl)ethenyl]benzo[1,2-*c*]1,2,5-oxadiazole (8*E*d). From the chromatographic purification process of **8*E*** was also isolated the deoxygenated analogue. Orange solid, mp 172.0–175.0 °C (Found: C, 72.1; H, 5.4; N, 15.5. $C_{16}H_{15}N_3O$ requires C, 72.4; H, 5.7; N, 15.8); ^{1}H NMR ($CDCl_3$) δ 3.05 (s, 6H), 6.75 (d, J = 8.8, 2H), 6.99 (d, J = 16.2, 1H), 7.22 (d, J = 16.2, 1H), 7.48 (d, J = 8.7, 2H), 7.64 (s, 1H), 7.75 (d, J = 9.5, 1H), 7.79 (d, J = 9.5, 1H); MS, *m*/*z* (abundance, %): 250 ($M^{+\cdot}-15$, 10), 208 (7), 132 (8), 166 (17), 57 (100); IR ν 2910, 1599, 1362, 872, 814.

5.3.8. 5*E*-[2-(4-Carboxyphenyl)ethenyl]benzo[1,2-*c*]1,2,5-oxadiazole N^1-oxide (10*E*). Yellow solid, mp 299.0–302.0 °C (Found: C, 63.9; H, 3.5; N, 9.8. $C_{15}H_{10}N_2O_4$ requires C, 63.8; H, 3.6; N, 9.9); ^{1}H NMR (DMSO-d_6) δ (ppm) 7.55 (d, J = 16.5, 1H), 7.63 (d, J = 17.0, 1H), 7.76 (d, J = 8.2, 2H), 7.79 (bs, 1H), 7.96 (bs, 2H), 7.99 (d, J = 8.2, 2H); MS, *m*/*z* (abundance, %): 282 ($M^{+\cdot}$, 10), 265 (15), 236 (20), 212 (100), 131 (60); IR ν 2548, 1670, 1610, 1292, 847.

5.3.9. 5*Z*-[2-(4-Carboxyphenyl)ethenyl]benzo[1,2-*c*]1,2,5-oxadiazole N^1-oxide (10*Z*). Yellow solid, mp 155.0–158.0 °C (Found: C, 63.8; H, 3.3; N, 9.6. $C_{15}H_{10}N_2O_4$ requires C, 63.8; H, 3.6; N, 9.9); ^{1}H NMR (DMSO-d_6) δ 6.84 (d, J = 12.3, 1H), 6.97 (d, J = 12.4, 1H), 7.07 (bs, 1H), 7.38 (d, J = 8.1, 2H), 7.54 (bs, 2H), 7.87 (d, J = 8.2, 2H); MS, *m*/*z* (abundance, %): 282 ($M^{+\cdot}$, 10), 265 (15), 236 (20), 212 (100), 131 (60); IR ν 2544, 1680, 1609, 1287, 887.

5.3.10. 5*E*-[2-(4-Cyanophenyl)ethenyl]benzo[1,2-*c*]1,2,5-oxadiazole N^1-oxide (11*E*). Orange-brown solid, mp 193.0–196.0 °C (Found: C, 68.2; H, 3.4; N, 15.9. $C_{15}H_9N_3O_2$ requires C, 68.4; H, 3.5; N, 16.0); ^{1}H NMR ($CDCl_3$) δ 7.50 (bs, 1H), 7.61 (bs, 1H), 7.62

(s, 2H), 7.68 (bs, 1H), 7.83 (d, $J = 8.3$, 1H), 7.86 (bs, 1H), 7.90 (d, $J = 8.4$, 2H); MS, *m*/*z* (abundance, %): 263 ($M^{+\cdot}$, 84), 247 (55), 230 (64), 215 (30), 203 (82), 190 (100), 177 (34); IR *v* 2222, 1615, 1525, 820.

5.3.11. 5*Z*-[2-(4-Cyanophenyl)ethenyl]benzo[1,2-*c*]1,2,5-oxadiazole *N*[1]-oxide (11*Z*). Yellow solid, mp 145.0–147.0 °C (Found: C, 68.1; H, 3.6; N, 15.8. $C_{15}H_9N_3O_2$ requires C, 68.4; H, 3.5; N, 16.0); ^{1}H NMR (DMSO-d_6) δ 6.94 (d, $J = 12.3$, 1H), 7.01 (d, $J = 12.4$, 1H), 7.18 (bs, 1H), 7.47 (bs, 2H), 7.54 (d, $J = 8.3$, 2H), 7.73 (d, $J = 8.3$, 2H); MS, *m*/*z* (abundance, %): 263 ($M^{+\cdot}$, 91), 247 (18), 230 (39), 215 (25), 203 (100), 190 (59), 177 (41); IR *v* 2228, 1607, 1520, 826.

5.3.12. 5*Z*/*E*-[2-(3-Fluorophenyl)ethenyl]benzo[1,2-*c*]1,2,5-oxadiazole *N*[1]-oxide (13*E*/*Z*). Yellow solid (Found: C, 65.3; H, 3.2; N, 10.5. $C_{14}H_9FN_2O_2$ requires C, 65.6; H, 3.5; N, 10.9); ^{1}H NMR ($CDCl_3$) δ 6.61 (d, $J = 12.2$, 1H), 6.84 (d, $J = 12.2$, 1H), 6.98 (m, 4H), 7.12 (d, $J = 16.5$, 1H), 7.21 (d, $J = 16.2$, 1H), 7.23–7.41 (m, 7H), 7.59 (bs, 3H); MS, *m*/*z* (abundance, %): 256 ($M^{+\cdot}$, 31), 240 (30), 196 (84), 183 (100), 170 (56), 146 (39); IR *v* 1611, 1582, 1524, 781, 681.

5.3.13. 5*Z*/*E*-[2-Cyclohexylethenyl]benzo[1,2-*c*]1,2,5-oxadiazole *N*[1]-oxide (15*E*/*Z*). Brown oil (Found: C, 68.4; H, 6.2; N, 11.1. $C_{14}H_{16}N_2O_2$ requires C, 68.8; H, 6.6; N, 11.5); ^{1}H NMR ($CDCl_3$) δ 1.25 (bs, 6H), 1.75 (bs, 5H), 5.70 (m, 1H), 6.25 (m, 1H), 7.20 (bs, 2H), 7.40 (bs, 1H); MS, *m*/*z* (abundance, %) 244 ($M^{+\cdot}$, 39), 228 (52), 166 (100); IR *v* 1655, 1437, 953, 708.

5.3.14. 5*E*-[2-(Methoxycarbonyl)ethenyl]benzo[1,2-*c*]1,2,5-oxadiazole *N*[1]-oxide (16*E*). Yellow-white solid, mp 140.0–143.0 °C (Found: C, 54.3; H, 3.6; N, 12.8. $C_{10}H_8N_2O_4$ requires C, 54.6; H, 3.7; N, 12.7); ^{1}H NMR ($CDCl_3$) δ 3.86 (s, 3H), 6.54 (d, $J = 16$, 1H), 7.50 (bs, 3H), 7.68 (d, $J = 16.0$, 1H); MS, *m*/*z* (abundance, %) 220 ($M^{+\cdot}$, 100), 204 (27), 189 (27), 173 (36), 145 (15); IR *v* 1721, 1613, 1578, 1198, 812.

5.4. 5*E*-[2-(4-Hydroxyphenyl)ethenyl]benzo[1,2-*c*]1,2,5-oxadiazole *N*[1]-oxide (9*E*)

5.4.1. 4Z/E-[2-(4-Chloro-3-nitrophenyl)ethenyl]phenol (V). A mixture of 4-chloro-3-nitrobenzaldeyde (300 mg, 1.60 mmol), the corresponding phosphonium salt **IId** (800 mg, 1.90 mmol), K_2CO_3 (520 mg, 3.80 mmol), 18-crown-6 (5 mg, 0.02 mmol), and DMF (10 mL) as solvent was stirred at 100–110 °C for 1.5 h. After the work-up, the residue was purified by column chromatography (SiO_2, petroleum ether/EtOAc (0–10%)), yellow solid (76 mg).

5.4.2. 5E-[2-(4-Hydroxyphenyl)ethenyl]benzo[1,2-*c*]1,2,5-oxadiazole *N*[1]-oxide (9E). A mixture of **V** (20.5 mg, 0.08 mmol), NaN_3 (4.4 mg, 68 mmol), and DMSO (1 mL) as solvent was heated at 60–65 °C for 4 h and then at 80–90 °C for 3 h. After the work-up, the residue was purified by column chromatography (SiO_2, petroleum ether/EtOAc (0–20%)). Yellow solid (5 mg), mp 174.3–175.1 °C (Found: C, 65.9; H, 3.8; N, 10.8. $C_{14}H_{10}N_2O_3$ requires C, 66.1; H, 4.0; N, 11.0); ^{1}H NMR ($CDCl_3$) δ 6.92 (d, $J = 8.6$, 2H), 7.24 (d, $J = 16.4$, 1H), 7.47 (d, $J = 16.4$, 1H), 7.56 (d, $J = 8.6$, 2H), 7.60 (bs, 2H), 7.87 (bs, 1H), 8.68 (bs, 1H); MS, *m*/*z* (abundance, %) 254 (M^+, 48), 238 (7), 194 (72), 165 (100), 139 (20), 115 (59); IR *v* (cm^{-1}) 3400, 1715, 1655, 1540, 1458, 1396, 1482, 1450, 1213, 1113, 1080.

5.5. General procedure for the synthesis of 5-ethenylbenzofuroxan derivatives 12, 14, and 17–21

Synthesis of **IVb–f** *and* **20**. A mixture of **III** (1.0 equiv), the corresponding aldehyde (1.0 equiv), K_2CO_3 (1.0 equiv), 18-crown-6 (0.01 equiv), and THF (5 mL/mmol) as solvent was stirred at reflux until the carbonyl compounds were not present (SiO_2, petroleum ether/EtOAc (8:2)). After the work-up, the residue was purified by column chromatography (SiO_2, petroleum ether/EtOAc (9:1)).

Synthesis of 5-ethenylbenzofuroxan derivatives **12**, **14**, **17–19**, *and* **21**. The corresponding alkene (**IVb–f** or **20**) (1.0 equiv), HCl (c) (10.0 equiv), and ethanol (12 mL/mmol) as solvent were heated at reflux during 1–2 h. The reaction mixture was cooled at room temperature and ethanolic NaOH (0.16% w/v, 1.25 equiv) was added and an intense red solution was obtained. The mixture was cooled at 0 °C and aqueous solution of NaClO (2.8 M, 4.0 equiv) was added dropwise, and the reaction mixture was stirred during 30 min. After the work-up, the residue was purified by column chromatography (SiO_2, petroleum ether/EtOAc (9:1)).

5.5.1. 5*E*-[2-(2-Nitrophenyl)ethenyl]benzo[1,2-*c*]1,2,5-oxadiazole *N*[1]-oxide (12*E*). Yellow solid, mp 190 (d) °C (Found: C, 59.6; H, 3.0; N, 14.5. $C_{14}H_9N_3O_4$ requires C, 59.4; H, 3.2; N, 14.8); ^{1}H NMR ($CDCl_3$) δ 7.45 (d, $J = 16.3$, 1 H), 7.60–7.75 (bs, 3H), 7.82 (t, $J = 7.6$, 1H), 7.83 (d, $J = 16.2$, 1H), 7.91 (bs, 1H), 8.02 (d, $J = 7.7$, 1H), 8.07 (dd, $J = 1.2$, $J = 8.2$, 1H); MS, *m*/*z* (abundance, %): 283 ($M^{+\cdot}$, 25), 267 (5), 223 (6), 181 (10), 120 (19), 92 (95), 91 (100).

5.5.2. 5*Z*-[2-(2-Nitrophenyl)ethenyl]benzo[1,2-*c*]1,2,5-oxadiazole *N*[1]-oxide (12*Z*). Yellow solid, mp 135 (d) °C (Found: C, 59.2; H, 2.9; N, 14.6. $C_{14}H_9N_3O_4$ requires C, 59.4; H, 3.2; N, 14.8); ^{1}H NMR ($CDCl_3$) δ 6.77 (d, $J = 12.0$, 1H), 6.83–6.98 (bs, 1H), 7.16 (d, $J = 12.0$, 1H), 7.26 (m, 3H), 7.52 (m, 2H), 8.19 (m, 1H); MS, *m*/*z* (abundance, %) 283 ($M^{+\cdot}$, 79), 267 (1), 223 (4), 120 (13), 119 (100), 92 (86), 91 (25); IR *v* 3100, 1620, 1522, 1341, 1462, 793.

5.5.3. 5*E*-[2-(4-Bromophenyl)ethenyl]benzo[1,2-*c*]1,2,5-oxadiazole *N*[1]-oxide (14*E*). Orange solid, mp 170 (d) °C (Found: C, 52.8; H, 2.7; N, 8.6. $C_{14}H_9BrN_2O_2$ requires C, 53.0; H, 2.9; N, 8.8); ^{1}H NMR ($CDCl_3$) δ 7.09 (d, $J = 16.4$, 1H), 7.17 (d, $J = 16.3$, 1H), 7.42 (d, $J = 8.4$, 2H), 7.56 (d, $J = 8.4$, 2H), 7.30–7.65 (bs, 3H); MS, *m*/*z* (abundance, %): 302 ($M^{+\cdot} + 2$–16, 2), 300 ($M^{+\cdot}$−16, 1), 192 (13), 178 (6), 63 (100); IR *v* 3100, 2926, 1603, 1568, 1530, 1007, 961, 839.

5.5.4. 5*Z*/*E*-(1-Hexenyl)benzo[1,2-*c*]1,2,5-oxadiazole N^1-oxide (17*E*/*Z*). Red-brown oil (Found: C, 65.9; H, 6.3; N, 12.5. $C_{12}H_{14}N_2O_2$ requires C, 66.0; H, 6.5; N, 12.8); ^{1}H NMR ($CDCl_3$) δ 0.92 (t, 3H), 0.96 (t, 3H), 1.28–1.60 (m, 16H), 5.92 (td, 2H), 6.34 (m, 6H), 7.00–7.60 (bs, 12H); MS, *m*/*z* (abundance, %): 218 ($M^{+\cdot}$, 25), 202 (3), 158 (5), 149 (100); IR *v* 2929, 1650, 1525, 1450, 1337, 1223.

5.5.5. 5*E*-[2-(2-Thienyl)ethenyl]benzo[1,2-*c*]1,2,5-oxadiazole N^1-oxide (18*E*). Brown solid, mp 122.0–125.0 °C (Found: C, 58.9; H, 3.1; N, 11.3; S, 12.7. $C_{12}H_8N_2O_2S$ requires C, 59.0; H, 3.3; N, 11.5; S, 13.1); ^{1}H NMR ($CDCl_3$) δ (ppm) 6.89 (d, J = 16.0, 1H), 7.08 (dd, J = 1.5, J = 3.6 1H), 7.20 (d, J = 3.5, 1H), 7.33 (s, 1H), 7.37 (d, J = 16.0, 1H), 7.40 (bs, 1H), 7.54 (bs, 2H); MS, *m*/*z* (abundance, %): 244 ($M^{+\cdot}$, 52), 228 (26), 184 (100), 171 (34), 139 (42); IR *v* 1622, 1570, 945, 702.

5.5.6. 5*E*-[2-(5-Nitro-2-thienyl)ethenyl]benzo[1,2-*c*]1,2,5-oxadiazole N^1-oxide (19*E*). Orange solid, mp 160 (d) °C (Found: C, 49.6; H, 2.4; N, 14.4; S, 10.8. $C_{12}H_7N_3O_4S$ requires C, 49.8; H, 2.4; N, 14.5; S, 11.1); ^{1}H NMR ($CDCl_3$) δ 7.42 (d, J = 4.3, 1H), 7.54 (d, J = 16.2, 1H), 7.63–7.80 (bs, 1H), 7.76 (d, J = 16.2, 1H), 7.80–7.95 (bs, 2H), 8.03 (d, J = 4.3, 1H); MS, *m*/*z* (abundance, %): 289 ($M^{+\cdot}$, 2), 148 (3), 140 (4), 128 (100), 102 (13); IR *v* 1611, 1572, 1524, 1329, 812, 731.

5.5.7. 5*Z*-[2-(4-Acetylamino-3-nitrophenyl)ethenyl]benzo-[1,2-*c*]1,2,5-oxadiazole N^1-oxide (20*Z*). Yellow solid, mp 134.0–135.0 °C (Found: C, 56.6; H, 3.5; N, 16.2. $C_{16}H_{12}N_4O_5$ requires C, 56.5; H, 3.6; N, 16.5); ^{1}H NMR ($CDCl_3$) δ 2.31 (s, 3H), 6.71 (d, J = 12.1, 1H), 6.79 (d, J = 12.1, 1H), 7.05 (bs, 1H), 7.34 (bs, 2H), 7.51 (dd, J = 1.9, J = 8.8, 1H), 8.11 (d, J = 1.9, 1H), 8.75 (d, J = 8.8, 1H), 10.34 (bs, 1H); MS, *m*/*z* (abundance, %) 340 ($M^{+\cdot}$, 3), 324 (44), 282 (100), 252 (18), 205 (35); IR *v* 3343, 1698, 1620, 1570, 1337.

5.5.8. 5*Z*-[2-Benzofurazanyl]benzo[1,2-*c*]1,2,5-oxadiazole N^1-oxide (21*Z*). Orange-brown solid, mp 125.0–128.0 °C (Found: C, 59.7; H, 2.9; N, 19.7. $C_{14}H_8N_4O_3$ requires C, 60.0; H, 2.9; N, 20.0); ^{1}H NMR ($CDCl_3$) δ 6.84 (d, J = 12.3, 1H), 6.92 (d, J = 12.3, 1H), 7.08 (bs, 1H), 7.26 (d, J = 9.3, 1H), 7.37 (bs, 2H), 7.74 (s, 1H), 7.77 (d, J = 9.4, 1H); MS, *m*/*z* (abundance, %): 280 ($M^{+\cdot}$, 14), 264 (23), 217 (46), 204 (37), 190 (100), 177 (46); IR *v* 1609, 1526, 1009, 885.

5.6. 5*E*-[2-(4-Pyridinyl)ethenyl]benzo[1,2-*c*]1,2,5-oxadiazole N^1-oxide (22*E*)

A mixture of 5-formylbenzofuroxan (0.2 g, 1.22 mmol), 4-picoline (0.12 mL, 1.22 mmol), and Ac_2O (10 mL) was heated at reflux during 4 h. After the work-up, the residue was purified by column chromatography (SiO_2, petroleum ether/EtOAc (8:2)). Brown solid, mp 180.0–181.5 °C (Found: C, 65.1; H, 3.6; N, 17.4. $C_{13}H_9N_3O_2$ requires C, 65.3; H, 3.8; N, 17.6); ^{1}H NMR ($CDCl_3$) δ 7.40 (bs, 3H), 7.30 (m, 2H), 7.80 (d, J = 15.0, 1H), 7.91 (d, J = 15.0, 1H), 8.71 (d, J = 9.0, 2H); MS, *m*/*z* (abundance, %): 239 ($M^{+\cdot}$, 32), 223 (97), 192 (100), 178 (71); IR *v* 1612, 1593, 1412, 964, 844, 750.

5.7. SAR

Structural manipulations were performed using Spartan'04 package. Structures discussed within this study were modeled using standard bond lengths and angles, and energy-minimized as implemented in the Spartan'04 software package, 1.0.1 version. On the more flexible molecules we performed the corresponding conformational analysis using the MM methods (Conformational Distribution module implemented in Spartan'04 package). All the compounds were built as the 6-substituted tautomers and as *Z*- or *E*-isomers. When the isomers' mixture was biologically evaluated the *E*-form was used in the SAR study. The conformer of minimum energy was fully optimized using B3LYP/6-31G*//AM1.

5.8. Biology

5.8.1. In vitro anti-trypanosomal activity. *Trypanosoma cruzi* epimastigotes (Tulahuen 2, CL Brener, and Y strains) were grown at 28 °C in an axenic medium (BHI-Tryptose) as previously described,[12–15] complemented with 5% fetal calf serum. Cells were harvested in the late log phase, resuspended in fresh medium, counted in Neubauer's chamber, and placed in 24-well plates (3×10^6/mL). Cell growth was measured as the absorbance of the culture at 610 nm, which was proved to be proportional to the number of cells present.[42] Before inoculation, the media were supplemented with the indicated amount of the studied compound from a stock solution in DMSO. The final concentration of DMSO in the culture media never exceeded 0.8% and the control was run in the presence of 0.8% DMSO and in the absence of any compound. No effect on epimastigotes' growth was observed by the presence of up to 1% DMSO in the culture media. The percentage of growth inhibition was calculated as follows: $PGI = \{1 - [(A_p - A_{0p})/(A_c - A_{0c})]\} \times 100$, where $A_p = A_{600}$ of the culture containing the compound at day 5; $A_{0p} = A_{600}$ of the culture containing the compound right after addition of the inocula (day 0); $A_c = A_{600}$ of the culture in the absence of any compound (control) at day 5; $A_{0c} = A_{600}$ in the absence of the compound at day 0. To determine IC_{50} values, parasite growth was followed in the absence (control) and presence of increasing concentrations of the corresponding compound. The IC_{50} values were determined as the compound concentration required to reduce by half the absorbance of the control (without compound).

5.8.2. In vitro cytotoxicity to macrophages. THP-1 human monocyte-like cells (ATCC, USA) were seeded (100.000 cells/well) in 96-well flat-bottomed microplates (Nunclon) and differentiated to macrophages by culture (5% CO_2, 37 °C, 48 h) in the presence of 50 ng/mL phorbol-12-myristate-13 acetate (Sigma) in RPMI 1640 medium supplemented with 10% heat-inactivated fetal calf serum. Afterward, cells were exposed for 48 h to the compounds (25.0–400.0 μM) or vehicle for control. Cell viability was then assessed by measuring the

mitochondrial-dependent reduction of 3-[4,5-dimethylthiazol-2-yl]-2,5-diphenyltetrazolium bromide (MTT, Sigma) to formazan. For that purpose, cells were washed with PBS and incubated (37 °C) with MTT 0.4 mg/mL for 3 h. Formazan was dissolved with DMSO (180 μL) and optical densities were measured at 560 nm. Each concentration was assayed three times and six additional controls (cells in medium) were used in each test. Cytotoxicity percentages (% C) were determined as follows: $\%\ C = [100 - (ODc - ODcm)/(ODc - ODvm)] \times 100$, where ODc is the mean of OD_{560} obtained for cells incubated with medium (controls), ODcm is the mean of OD_{560} cells incubated with different compound concentrations, and ODvm is the mean of OD_{560} of cells incubated with vehicle. The IC_{50}, macrophage values were determined as the drug concentration required to reduce by half the absorbance of the control.

Acknowledgments

This work received financial support from Fondo Clemente Estable (Uruguay), CSIC/UdelaR (Uruguay), and Collaborative Project UdelaR (Uruguay)—CSIC (Spain) (#2004UY0009). The macrophage's cytotoxicity studies were performed as part of a D.N.D.i. (Drugs for Neglected Disease initiative) Project.

References and notes

1. World Health Organization, <http://www.who.int/ctd/chagas>.
2. Moncayo, A. In *WHO Special Program for Research and Training in Tropical Diseases (TDR)*; World Health Organization Ed., Eleventh Programme Report of the UNPD: World Bank: Geneva, 1993; pp 67–75.
3. De Souza, W. *Curr. Pharm. Des.* **2002**, *4*, 269.
4. Almeida-de-Faria, M.; Freymuller, E.; Colli, W.; Alves, M. *J. Exp. Parasitol.* **1999**, *92*, 263.
5. Faucher, J. F.; Baltz, T.; Petry, K. G. *Parasitol. Res.* **1995**, *81*, 441.
6. Tyler, K. M.; Engman, D. M. *Int. J. Parasitol.* **2001**, *31*, 472.
7. Urbina, J. A. *Curr. Pharm. Des.* **2002**, *8*, 287.
8. Cerecetto, H.; González, M. *Curr. Top. Med. Chem.* **2002**, *2*, 1185.
9. Docampo, R.; Moreno, S. N. J. In *Free Radicals in Biology*; Pryor, W. A., Ed.; Academic Press: New York, 1984; pp 243–288.
10. Viodé, C.; Bettache, N.; Narimantas, C.; Krauth-Siegel, R. L.; Chauvière, G.; Bakalara, N.; Périé, J. *Biochem. Pharmacol.* **1999**, *57*, 549.
11. Chauviere, G.; Bouteille, B.; Enanga, B.; de Albuquerque, C.; Croft, S. L.; Dumas, M.; Perie, J. *J. Med. Chem.* **2003**, *46*, 427.
12. Cerecetto, H.; Di Maio, R.; González, M.; Risso, M.; Saenz, P.; Seoane, G.; Denicola, A.; Peluffo, G.; Quijano, C.; Olea-Azar, C. *J. Med. Chem.* **1999**, *42*, 1941.
13. Aguirre, G.; Cerecetto, H.; Di Maio, R.; González, M.; Porcal, W.; Seoane, G.; Denicola, A.; Ortega, M. A.; Aldana, I.; Monge-Vega, A. *Arch. Pharm.* **2002**, *335*, 15.
14. Aguirre, G.; Boiani, L.; Cerecetto, H.; Di Maio, R.; González, M.; Porcal, W.; Thomson, L.; Tórtora, V.; Denicola, A.; Möller, M. *Bioorg. Med. Chem.* **2005**, *13*, 6324.
15. Aguirre, G.; Boiani, L.; Boiani, M.; Cerecetto, H.; Di Maio, R.; González, M.; Porcal, W.; Denicola, A.; Piro, O. E.; Castellano, E. E.; Sant'Anna, C. M. R.; Barreiro, E. J. *Bioorg. Med. Chem.* **2005**, *13*, 6336.
16. Olea-Azar, C.; Rigol, C.; Opazo, L.; Morello, A.; Maya, J. D.; Repetto, Y.; Aguirre, G.; Cerecetto, H.; DiMaio, R.; González, M.; Porcal, W. *J. Child. Chem. Soc.* **2003**, *48*, 77.
17. Olea-Azar, C.; Rigol, C.; Mendizábal, F.; Briones, R.; Cerecetto, H.; Di Maio, R.; González, M.; Porcal, W.; Risso, M. *Spectrochim. Acta A* **2003**, *59*, 69.
18. Olea-Azar, C.; Rigol, C.; Mendizábal, F.; Cerecetto, H.; Di Maio, R.; González, M.; Porcal, W.; Morello, A.; Repetto, Y.; Maya, J. D. *Lett. Drugs Des. Dev.* **2005**, *2*, 294.
19. Boden, R. M. *Synth. Commun.* **1975**, 784.
20. Mallory, F. B. *Organ. Synth.* **1957**, *37*, 74.
21. Shi, M.; Xu, B. *J. Org. Chem.* **2002**, *67*, 294.
22. Grayson, M.; Keough, P. T. *J. Am. Chem. Soc.* **1960**, *82*, 3919.
23. Hernández, P.; Merlino, A.; Gerpe, A.; Porcal, W.; Piro, O. E.; González, M.; Cerecetto, H. *Arkivoc* **2006**, *xi*, 128.
24. Gasco, A.; Boulton, A. J. In *Advances in Heterocycles Chemistry*; Katritzky, A. R., Boulton, A. J., Eds.; Wiley: New York, 1981; Vol. 29, pp 251–340.
25. Visentin, S.; Amiel, P.; Fruttero, R.; Boschi, D.; Roussel, C.; Giusta, L.; Carbone, E.; Gasco, A. *J. Med. Chem.* **1999**, *42*, 1422.
26. Ermondi, G.; Visentin, S.; Boschi, D.; Fruttero, R.; Gasco, A. *J. Mol. Struct.* **2000**, *523*, 149.
27. Filardi, L. S.; Brener, Z. *Trans. R. Soc. Trop. Med. Hyg.* **1987**, *81*, 755.
28. Molina, J.; Brener, Z.; Romanha, A. J.; Urbina, J. A. *J. Antimicrob. Chem.* **2000**, *46*, 137.
29. Muelas, S.; Di Maio, R.; Cerecetto, H.; Seoane, G.; Ochoa, C.; Escario, J. A.; Gómez-Barrio, A. *Folia Parasitol.* **2001**, *48*, 105.
30. Hansch, C.; Leo, A. In *Exploring QSAR. Fundamentals and Applications in Chemistry and Biology*, Ed. American Chemical Society, Washington, 1995.
31. Hansch, C.; Leo, A.; Hoekman, D. In *Exploring QSAR. Hydrophobic, Electronic and Steric Constants*, Ed. American Chemical Society, Washington, 1995.
32. Myers, R. H. In *Classical and Modern Regression with Application*; P.W.S. Publishers: Boston, 1986.
33. Draper, N. R.; Smith, H. In *Applied Regression Analysis*, 2nd ed.; Wiley: New York, 1981.
34. Hehre, W. J.; Radom, L.; Schleyer, P. v. R.; Pople, J. A. In *Ab initio molecular orbital theory*; Wiley: New York, 1986.
35. Hehre, W. J.; Shusterman, A. J.; Huang, W. W. In *A Laboratory Book of Computational Organic Chemistry*; Wavefunction Inc.: California, 1996.
36. Becke, A. D. *Phys. Rev. A* **1988**, *38*, 3098.
37. Becke, A. D. *J. Chem. Phys.* **1993**, 5648.
38. Lee, C.; Yang, W.; Parr, R. G. *Phys. Rev. B Condens. Matter* **1988**, *37*, 785.
39. Spartan'04; Wavefunction, Inc. 18401 Von Karman Avenue, Suite 370. Irvine, California 92612 USA.
40. Cerecetto, H.; Dias, E.; Di Maio, R.; González, M.; Pacce, S.; Saenz, P.; Seoane, G.; Suescun, L.; Mombrú, A.; Fernández, G.; Lema, M.; Villalba, J. *J. Agric. Food Chem.* **2000**, *48*, 2995.
41. Boiani, M.; Cerecetto, H.; González, M.; Risso, M.; Olea-Azar, C.; Piro, O. E.; Castellano, E. E.; López de Ceráin, A.; Ezpeleta, O.; Monge-Vega, A. *Eur. J. Med. Chem.* **2001**, *36*, 771.
42. Denicola, A.; Rubbo, H.; Rodríguez, D.; Radi, R. *Arch. Biochem. Biophys.* **1993**, *304*, 279.